

Metallic Triple Beam Resonator with Thick-film Printed Drive and Pickup

T. Yan¹, B. E. Jones¹, R. T. Rakowski¹, M. J. Tudor², S. P. Beeby² and N. M. White²

¹The Brunel Centre for Manufacturing Metrology, Brunel University, Uxbridge, Middlesex UB8 3PH, UK
Email: barry.jones@brunel.ac.uk <http://www.brunel.ac.uk/research/bcmm/remise/index.htm>

²Department of Electronics and Computer Science, University of Southampton, Highfield, Southampton, Hampshire, SO17 1BJ, UK

Summary: *A triple beam resonator fabricated in 430S17 stainless steel with thick-film piezoelectric elements to drive and detect the vibrations is presented. The resonator substrate was fabricated by a simultaneous, double-sided photochemical etching technique and the thick-film piezoelectric elements were deposited by a standard screen-printing process. The combination of these two batch-fabrication processes provides the opportunity for mass production of the device at low cost. The resonator, a dynamically balanced triple beam tuning fork (TBTF) structure 23.5 mm long and 6.5 mm wide, has a favoured mode at 4.96 kHz with a Q-factor of 3630 operating in air.*

Keywords: *thick-film, piezoelectric, metallic resonator, triple beam tuning fork*

Category: *4 (Non-magnetic physical devices)*

1 Introduction

The thick film printing process has been successfully used to deposit piezoelectric materials onto silicon structures for fabrication of a silicon single beam resonator and other silicon devices [1]. More recently, this process has been applied to the fabrication of a metallic triple beam resonator [2]. This paper describes the design of the thick-film PZT-metallic triple beam resonator, the application of the thick-film printing technology in its fabrication and the results from the device. This device, a metallic triple beam tuning fork structure with thick-film printed piezoelectric drive and pickup elements, is the first of its kind [3]. The substrate of the resonator is fabricated by an inexpensive conventional photochemical etching process. The combination of processes used in the resonator fabrication presents low cost techniques for mass batch production of the device, in particular the use of thick-film screen-printing presents a large step forward for depositing the piezoelectric materials.

The thick-film screen-printing deposits relatively thick layers of material, typically between 50 μm and 100 μm . These films are capable of providing large excitation forces and detection signals when compared to alternative thin film piezoelectric materials. The piezoelectric properties of the thick film are generally also improved over the thin film alternatives [4]. The magnitude of the PZT element output depends upon the piezoelectric properties of the deposited layer, its thickness and the stress or voltage applied. Finite element analysis (FEA) is employed to simulate the modal behaviour with stress distribution of the resonator and to optimise the positioning of the PZT elements.

The triple beam tuning fork structure used in the resonator design is inherently more dynamically

balanced when compared to the single beam structure for the flexural resonator design. Such structures dissipate less energy through their supports and therefore possess an intrinsically higher mechanical quality factor (Q-factor).

2 Resonator design

The resonator consists of three beams (tines) aligned in parallel alongside each other and joined at a decoupling zone at each end which is in turn connected to the surrounding material. The central beam is twice the width of the two outer beams. The resonating element has a length of 23.5 mm, a thickness of 0.25 mm and beam widths of 2 mm and 1 mm. The distance between the beams is 0.5 mm. Finite element analysis (FEA) has been performed to predict the modal behaviour with stress distribution and eigenfrequencies of the resonator. Thick-film PZT elements were printed on separate regions at each end of the central beam, where maximum stresses exist as the resonator operates in its favoured mode of vibration. The PZT element at one end drives the vibrations, whilst the PZT element on the other end detects them. Positioning the PZT driving and sensing elements on the regions of maximum stresses maximises the degree of mechanical coupling between the active piezoelectric layer and the resonator for generation of both driving forces and sensing signals. Figure 1 shows a plan view of the resonator design. Large earth regions in the fields surrounding the drive and detect electrodes were included in order to minimise cross talk between the drive port and the detect port [5].

The triple beam resonator has three different fundamental modes of vibration out of the plane of the wafer. In mode one, the three tines oscillate in phase. In mode two, the central tine does not oscillate

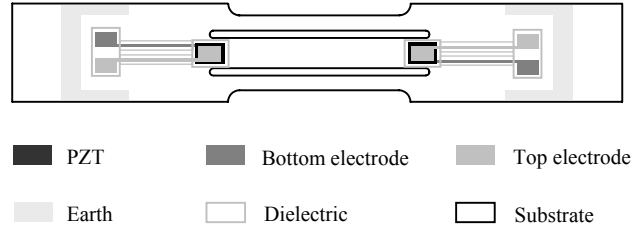


Fig.1. A plan view of the resonator structure with PZT drive and detection elements.

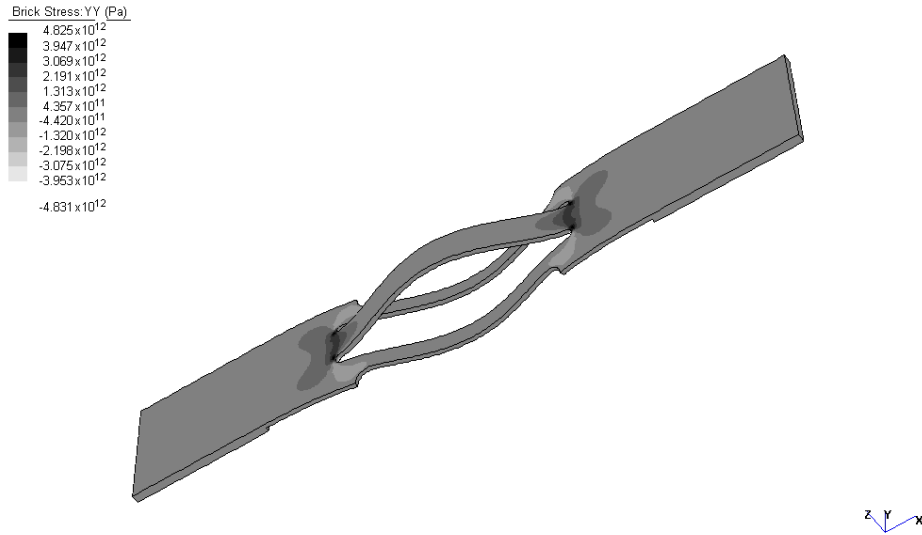


Fig.2. A stress contour plot for the resonator in mode 3 modelled by FEA.

while the outer tines vibrate at a phase of 180° with respect to each other. In mode three, the central tine vibrates in anti-phase with the outer tines. This mode is the optimum mode for operating such a triple beam resonator, as both bending moments and shearing forces at the decoupling zone are cancelled out and very little vibration energy is coupled into the supporting frame at each end. This improves the Q factor of the device and therefore the performance of a resonant sensor employing such a device. The in-phase mode has the lowest resonant frequency, followed by the second and the third modes. There are also other higher-order modes of vibration. Figure 2 shows a stress contour plot for the modelled resonator vibrating in mode 3. This gives an indication of the stress distribution along the resonator as it oscillates in this mode. The values calculated were not actual stresses, but providing a graphical representation of the regions of maximum stresses. The FEA calculated natural frequency for mode 3 was 5.51 kHz. This is an approximation since it ignores the presence of the PZT elements which will increase the natural frequency by increasing the stiffness of the structure at the roots of the beam, and contrarily, the firing (annealing) of the beam during thick-film printing process which will decrease the natural frequency by decreasing the Young's modulus of the beam material.

3 Fabrication

The substrate of the resonator was fabricated from a 0.5 mm thick 430S17 stainless steel thin sheet using a simultaneous double-sided photochemical etching technique. The top pattern defined the layout of the resonator and the bottom pattern etched in a standoff distance leaving the section of resonating element 0.25 mm thick. A dielectric layer was then deposited at the defined driving and sensing regions on the top surface of the resonator using a standard screen-printing process, and consecutively layers of bottom gold electrode, piezoelectric paste and top gold electrode were deposited each with their own screens. The dielectric layer was required to isolate the bottom electrode from the resonator substrate to enable polarisation of the piezoelectric layer at a later stage. Figure 3 illustrates the process of fabrication.

During printing, the thick-film paste is spread across the surface of a patterned screen and a squeegee is drawn across the screen bringing it down into contact with the substrate and pressing the paste through the open areas in the screen. As the squeegee passes, the screen snaps back to its original position and the paste remains deposited on the substrate surface. This process has been successfully applied to print thick-film piezoelectric elements onto a silicon micromechanical resonator as small as 2000 μm long,

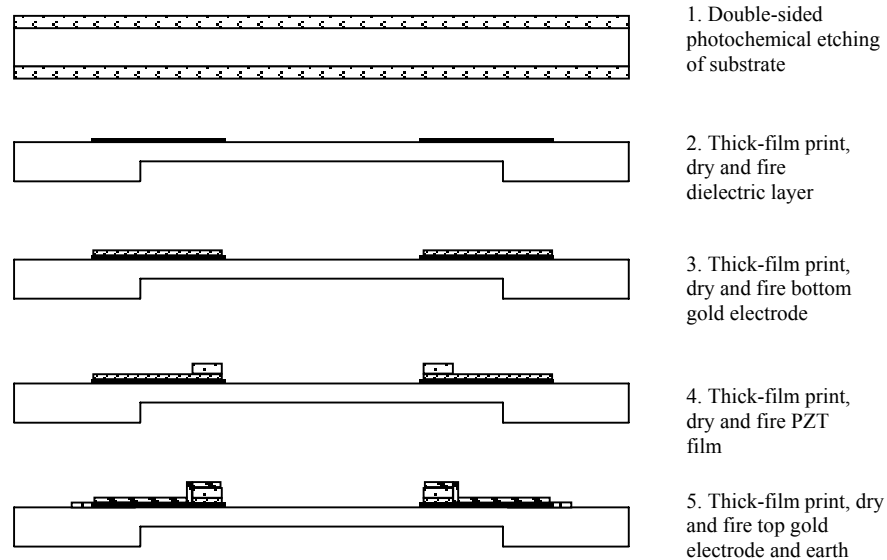


Fig.3. Schematic of resonator fabrication process.

520 μm wide and 30 μm thick [1].

The PZT paste was prepared from 6 μm average grain size, 95% PZT-5H powder, 5% lead borosilicate powder, and approximately 5ml ESL 400 organic vehicle per 20 g powder mix. This was blended thoroughly using a triple roll mill to ensure adequate particulate dispersion. The lead borosilicate was added to act as a binder. During a later firing stage the lead borosilicate melts, the fine powders sinter and the overall film becomes a solid composite material. The function of the lead borosilicate is to bond the film to the substrate and also to bind the active particles together. The organic vehicle was needed in order to produce the correct viscosity of paste for screen-printing and it can be removed during a later drying stage before firing.

The prepared PZT paste was printed through a stainless steel screen of mesh density 250 wires per inch orientation at 45° to the frame and patterned with a 23 μm thick layer of emulsion, using a Dek 1750 RS printer. Two print strokes were carried out which yielded a thickness of approximately 50 μm after drying and firing. The printed film was then dried at 140 $^\circ\text{C}$ in a Dek model 1209 infra-red dryer and fired on a belt furnace for 1 hour, being held at a peak temperature of 850 $^\circ\text{C}$ for 20 min, which has been found to sinter the particles adequately. After drying, the film retains a rigid pattern on the substrate and is relatively immune to smudging; another layer can be printed directly onto the dry film. Various combination of printing-drying-printing-drying-firing can be performed if the film thickness in excess of 50 μm is required. After firing, the film is firmly attached to the substrate and further screen-printed layers can be added as required.

A dielectric composition ink, ESL 8986, was used to print the dielectric layer and a gold cermet ink, ESL 8836, was used to print the bottom and top electrode

layers, each with one print stroke leaving an approximate thickness of 25 μm for each layer. These were dried and fired with the same profile used for the PZT. The printed PZT layer is sandwiched between two electrodes thereby forming a capacitor structure, the dielectric layer being the widest on the substrate and the gold top electrode being 50 μm smaller in all directions than the PZT pattern to prevent short circuit.

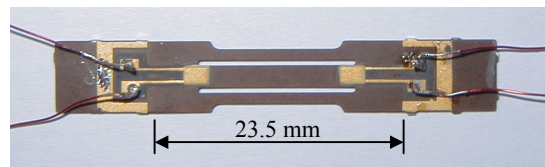


Fig.4. Photograph of the metallic resonator.

The fabricated resonators were sawn from the wafer and the wires were soldered on to the electrode pads. A photograph of the metallic resonator is shown in Figure 4. The PZT elements were then connected in parallel and poled for one hour at 130 $^\circ\text{C}$ with a voltage of 200 V across the electrodes. Given the measured PZT layer thickness of 50 μm , an electric field of strength 4 MV/m was generated during the polarising process. This aligns the dipoles within the PZT material thereby bestowing its piezoelectric properties.

3 Resonator operation and results

The resonator operating in air was first tested in an open-loop configuration in order to observe the vibration modes and confirm successful operation of the driving and sensing mechanisms. The PZT element at one end of the resonator was driven by an AC signal of 1V pk-pk from a Hewlett-Packard 89410A Vector Signal Analyser with the tracking

generator scanning over a frequency range of 1-8 kHz. The PZT element on the other end of the resonator was connected to a Kistler 5011 Charge Amplifier and the output from the charge amplifier was fed back to the signal analyser for frequency response analysis of the resonator. Figure 5 shows the frequency response of the resonator with a dominant resonance at 4.96 kHz and three other resonances visible at frequencies 1.57 kHz, 3.68 kHz and 6.62 kHz. From the FEA simulations, these resonances correspond to the third, the first, the second and the fourth vibration modes of the resonator respectively. The third mode of vibration is markedly dominant due to the favourable dynamic structural balance associated with this mode. The blown-up inset in the figure is the response for the third mode.

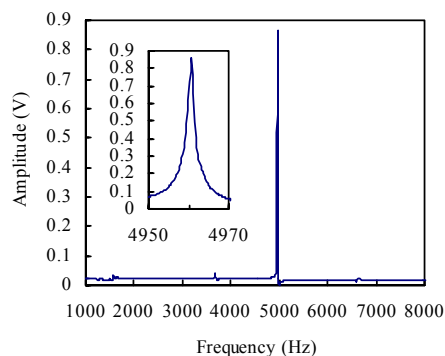


Fig.5. Amplitude-frequency response of the resonator.

The Q factor of the resonator in air for mode three was measured to be 3630. This is excellent when compared to other reported Q-factors for resonant structures vibrating in air. For example, a Q-factor of 70 was reported for a silicon single beam resonator with PZT thick film drive/detection elements [1], a Q-factor of 400 for a silicon triple beam resonator with thin film drive and detection [6], a Q-factor of 140 for a metallic double-beam-tuning-fork resonator with bulk PZT elements [7] and a Q-factor of 740 for a metallic triple-beam-tuning-fork resonator with bulk PZT drive and detection [8].

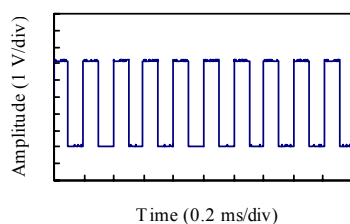


Fig.6. Frequency output of the resonator in closed-loop.

Next, the resonator was tested, again at atmospheric pressure, in a feedback closed-loop configuration. The PZT sensing element was connected to a charge amplifier circuit, followed by a digital 90-degree phase shift circuit and a second stage of amplification all on one circuit board. The output from the second stage amplification was fed back to the drive PZT element. In such a way, the resonator was maintained at resonance in the required favourable mode of

oscillation. Figure 6 shows the frequency output of the resonator in such a closed-loop operation.

4 Conclusions

This paper has reported a metallic triple beam resonator etched from stainless steel in which the vibrations are driven and detected by thick-film printed piezoelectric elements. The resonator has been characterised in an open-loop test which identified the modes of vibration and confirmed the successful operation of the device and of the driving and sensing mechanisms. The resonator has further successfully been operated in a closed-loop configuration with the designed associated electronics. The presented resonator has shown a good mode selectivity with a Q factor of 3630 operating in air, which compares very favourably with other reported resonators of similar structures operating in air. This device can be easily mass-produced at low cost for use in a wide range of measuring systems, for example load cells, weighing machines, torque transducers and pressure sensors. Details of characteristics, interfacing and other sizes/material configurations are under investigation.

Acknowledgements

The authors wish to acknowledge the support of EPSRC (Grant GR/R51773) and the industrial collaborators within the Intersect Project (2002-2005) entitled "Resonant Microsensor Modules for Measurement of Physical Quantities (REMISE)".

References

- [1] S. P. Beeby and N. M. White. Silicon micromechanical resonator with thick-film printed vibration excitation and detection mechanisms. *Sens. Actuators A* 88 (2001) 189-197.
- [2] T. Yan, B. E. Jones, R. T. Rakowski, M. J. Tudor, S. P. Beeby and N. M. White. Thick-film PZT-metallic triple beam resonator. To appear in *Electron. Lett.* (2003).
- [3] B. E. Jones and N. W. White. Metallic resonators. Patent Application GB0302585-5 (2003).
- [4] S. P. Beeby, A. Blackburn and N. M. White. Processing of PZT piezoelectric thick films on silicon for microelectromechanical systems. *J. Micromech. Microeng.* 9 (1999) 218-229.
- [5] C. J. van Mullem, H. A. C. Tilmans, A. J. Moushaan and J. H. J. Fluitman. Electrical cross-talk in two-port resonators – the resonant silicon beam force sensor. *Sens. Actuators A* 31 (1992) 168-173.
- [6] Th. Fabula, H. -J. Wagner and B. Schmidt. Triple-beam resonant silicon force sensor based on piezoelectric thin films. *Sens. Actuators A* 41-42 (1994) 375-380.
- [7] C. Barthod., Y. Teisseyre, C. Gehin and G. Gautier. Resonant force sensor using a PLL electronic. *Sens. Actuators A* 104 (2003) 143-150.
- [8] D. S. Randall, M. J. Rudkin, A. Cheshmehdoost and B.E. Jones. A pressure transducer using a metallic triple-beam tuning fork. *Sens. Actuators A* 60 (1997) 160-162.